Aptisi Transactions on Technopreneurship (ATT)
Vol. 4 No. 3 November 2022

P-ISSN: 2655-8807
E-ISSN: 2656-8888

The Use of TensorFlow in Analyzing Air Quality Artificial Intelligence Predictions $PM_{2.5}$

Untung Rahardja[1], Qurotul Aini[2], Po Abas Sunarya[3], Danny Manongga[4], Dwi Julianingsih[5]
Magister of Information Technology[1,2,4],
Master in Management[3],
Department of Retail Management[5]
University of Raharja[1,2,3,5], Satya Wacana Christian University[4]
Jl. Jenderal Sudirman No.40, Cikokol, Kec. Tangerang, Kota Tangerang, Banten 15117[1,2,3,5]
Jl. Diponegoro No.52-60, Salatiga, Kec. Sidorejo, Kota Salatiga, Jawa Tengah 50711[4]
e-mail: untung@raharja.info[1], aini@raharja.info[2], abas@raharja.info[3], danny.manongga@uksw.edu[4], dwi.julianingsih@raharja.info[5]

Author Notification
18 October 2022
Final Revised
30 October 2022
Published
31 October 2022

To cite this document:
Rahardja, U. ., Aini, Q. ., Sunarya, P. A. ., Manongga, D. ., & Julianingsih, D. (2022). The Use of TensorFlow in Analyzing Air Quality Artificial Intelligence Predictions PM2.5. Aptisi Transactions on Technopreneurship (ATT), 4(3), 313–324.

DOI: https://doi.org/10.34306/att.v4i3.282

Abstract

Artificial intelligence techniques to forecasts based on the Community Multiscale Air Quality ($PM_{2.5}$) operational model can be known using TensorFlow. TensorFlow was used in this study to assess the scores of the Recurrent Neural Networks (RNN) input variables on the 6-hour forecast for July-October 2022. The relevance scores for the one- and two-day forecasts are represented by the sum of the relevance scores across the target prediction timeframe 2–5 and 4–7 previous time steps. The initial selection of input variables was based on their correlation coefficient with the measured $PM_{2.5}$ concentration. Still, the order of contribution of the input variables measured by TensorFlow was different from the order of their correlation coefficients, which indicated an inconsistency between the linear and nonlinear variables of the method. It was found that the retraining of the RNN model using a subset of variables with a high relevance score resulted in a predictive ability similar to the initial set of input variables. By using TensorFlow to decode the black box artificial intelligence model, this research can help improve the RNN prediction model. The novelty in this study is that the Artificial Intelligence (AI) model of TensorFlow can use challenging decision-making processes to explain using our current understanding or simple linear ideas. Thus a more profound knowledge of the mechanisms associated with $PM_{2.5}$ concentration, which continues to be a vital issue for this field of research, will be required to understand the drivers of decision-making in Artificial Intelligence (AI) models, particularly in TensorFlow.

Keywords: *Artificial Intelligence, Air Quality, TensorFlow, RNN, $PM_{2.5}$*

1. Introduction

The dangerous air pollutant known as $PM_{2.5}$, which has an aerodynamic diameter of 2.5 µgram/m^3, is responsible for substantial economic losses as well as respiratory and cardiovascular illnesses. Since 2017, the National Institute of Environmental Research (NIER) of the Indonesia has been forecasting $PM_{2.5}$ levels in recognition of the severely harmful impacts

of $PM_{2.5}$ [1],[2]. In March 2018, the $PM_{2.5}$ air quality limits were raised. Despite stronger laws, Tangerang's yearly average $PM_{2.5}$ concentration has maintained at 25 µgram/m^3, which is far higher than the 10 µgram/m^3 annual average recommended by the World Health Organization. Due to the buildup of air pollutants brought into Indonesia from continental sources to the west of Indonesia, record-breaking $PM_{2.5}$ concentrations (peak >150 µgram/m^3) were detected in Tangerang in July-October 2022. For high $PM_{2.5}$ events ($PM_{2.5}$ 36 µgram/m^3) in 2021, NIER's one-day prediction accuracy was only 56% [3],[4],[5].

By supplementing the Community Multiscale Air Quality (CMAQ) model's forecasts starting in 2021 with artificial intelligence (AI) techniques, the NIER recommended enhancing the $PM_{2.5}$ prediction accuracy. In order to match the operational forecasting schedule of NIER, Created a recurrent neural network (RNN) model that forecasts $PM_{2.5}$ concentrations up to 2 days at 6-h intervals [6],[7],[8]. The RNN model is quick enough for real-time operational forecasting, and depending on the forecast lead time [9],[10],[11], the RNN-based prediction accuracy ranges from 74 to 80% (11% to 18% better than the CMAQ-based forecast). The CMAQ-based $PM_{2.5}$ estimations are improved by the RNN model, but it is impossible to determine the exact steps that each input variable took to influence the prediction or the relative weight that each input variable had [12],[13]. It is challenging to comprehend the intricate prediction processes since AI might make decisions differently from humans. Forecasting professionals are generally skeptical about the veracity of AI-based forecast findings due to the opaqueness of the AI model [14],[15].

The concept of eXplainable Artificial Intelligence (XAI), which was just proposed, can serve as the foundation for tracking the steps taken to produce prediction outcomes and for disguising the black box of AI models [16],[17]. By removing the causes of inaccuracy and gaining new pertinent knowledge from AI, XAI can, in particular, reveal a causal relationship between the input and output variables to enhance models [18],[19]. One of the most popular strategies for handling regression issues in XAI-related studies is layer-wise relevance propagation (TensorFlow) [20],[21]. Back propagation is used to spread a relevance score, which in TensorFlow stands for the contribution of a neuron to the output, across all layers of a neural network [22],[23],[24]. Speech recognition, therapy prediction, computer security, and Alzheimer's disease detection are just a few of the areas where TensorFlow has been used [25],[26].

Using the TensorFlow method to examine the inner workings of the existing RNN model, this study seeks to find the most significant input variables in forecasting $PM_{2.5}$ in the Tangerang metropolitan area of Indonesia. This study concentrated on the winter season because it is when average $PM_{2.5}$ concentrations and high-$PM_{2.5}$ episode frequency are both at their maximum (July-August-September). By comparing relevance scores obtained from the TensorFlow to timesteps and covariates, we evaluated their contributions to $PM_{2.5}$ prediction [27],[28],[29]. The RNN model was retrained and tested using only the timesteps and variables with high relevance scores to see if the primary input time-steps and variables provided by the TensorFlow had significantly contributed to the prediction [30],[31],[32]. The structure of this document is as follows. The RNN forecasting system and TensorFlow's data and methodology are explained in Section 2 of this article. The results based on the TensorFlow are presented in Section 3. A discussion of the findings and a summary are provided in Section 4.

2. Research Method

In this study, we are using Tensorflow, where TensorFlow is an open-source library created by the Google Brain team, usually used for numerical computing and large-scale machine learning [33],[34],[35]. Thus, this gives the author an advantage in using the TensorFlow method, which can train and run a neural network to classify handwriting, recognize images/objects, and combine words.

2.1 Data

During July-October 2022, data from RNN simulations with input from observations and numerical models at 6-h intervals were gathered for the Tangerang metropolitan area in Indonesia, including Tangerang and Semarang cities, North and South Tangerang provinces (Fig. 1). The data collected included atmospheric variables from 9 Automated Surface Observing System (ASOS) stations in the Tangerang metropolitan area (red circles in Fig. 1; 1,

3, and 2 stations at the four districts, respectively) and air pollutants from 112 ground stations (white circles in Fig. 1; 25, 15, 18, and 54 stations at the four districts, respectively). Each district's ground data and ASOS station data were averaged. During July-October 2022, data from RNN simulations with input from observations and numerical models at 6-h intervals were gathered for the Tangerang metropolitan area in Indonesia, including Tangerang and Semarang cities, North and South Tangerang provinces (Fig. 1).

Three-dimensional meteorological variables from the Weather Research and Forecasting (WRF) model running at a resolution of 27 km using baseline data based on the Meteorology, Climatology and Geophysics Agency (BMKG), back-track from the FLEXible PARTicle dispersion TensorFlow model, and air pollutant concentrations from the CMAQ model. are some of the input data used by the numerical model. The CMAQ and FLEXPART models were run using WRF simulated meteorological data. The 72-hour reverse trajectory starting at 500 meters above sea level above Tangerang is predicted by the BMKG with the aim of providing reliable and reliable meteorological, climatological, air quality and geophysical data, information and services. Coordinate and facilitate activities in the fields of meteorology, climatology, air quality and geophysics (www.bmkg.go.id/). The WRF and CMAQ models use the same physical and chemical parameters as the fast radiation transfer model, 6 class single moment WRF Schematic. Carbon bond gas phase chemistry scheme 05, Dudhia short radiation scheme, YSU planetary boundary layer Kain-Fritsch convective scheme, aerosol module AERO5, Euler backward iterative chemical solver, Yamo horizontal advection breaker, multiscale horizontal diffusion module, and eddy vertical diffusion module are some example of a convective scheme. Utilizing the Sparse Matrix Operator Kernel Emissions model, emission data is handled for the CMAQ simulation.

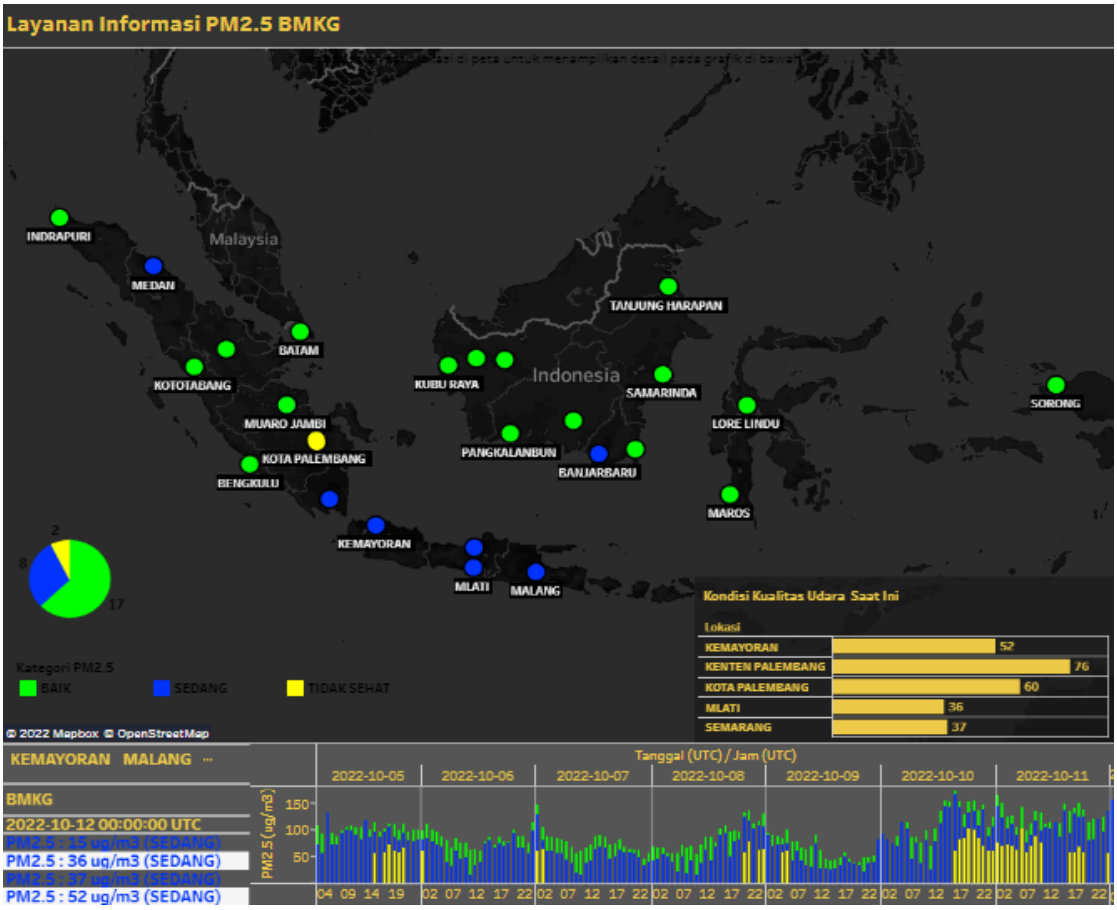

Figure 1. $PM_{2.5}$ Real Time Particulate
(Source: https://iklim.bmkg.go.id/id/)

Three different forms of input data for the RNN model were computed using the outputs of the numerical model. First, an average is calculated over the grid locations where each district is located using the predicted surface air quality variables and the meteorological variables at the four vertical levels (surface, 850 hPa, 700 hPa, and 500 hPa). The air quality characteristics predicted by the CMAQ model match those that were actually observed. Geopotential heights, air temperatures, relative humidity, horizontal and vertical winds, and other meteorological factors are all predicted. Second, the synoptic composite patterns for high-$PM_{2.5}$ occurrences were compared to the meteorological fields using one-dimensional cosine similarities, which show similarities between the two. Third, the path of the air pollutants was determined by grouping the back-trajectories into five clusters: south, local, long-northwest, short-northwest, and north. The agglomerative hierarchical clustering method was used to perform the categorization. The Euclidean distance approach was used to determine the likelihood of affinity to each cluster.

The RNN model's 21 simulated input variables and 11 observed input variables are correspondingly summarized in Tables 1 and 2. The observed $PM_{2.5}$ during the same period has correlation coefficients of >0.3 with all input variables, with the exception of the observed horizontal winds (U and V), precipitation (PRCP), and estimated probabilities of the five back-trajectory clusters (CP1-CP5). In example, the observation data's air quality variables exhibited high correlation values larger than 0.443, while in table 1 the meteorological variable has a relatively low correlation coefficient between 0.068 and 0.467. The correlation coefficients for the air quality variable and the meteorological variables in the numerical model data were both weaker than those in the observation data (Table 2), appearing in the ranges of 0.352 to 0.655 and 0.089 to 0.384, respectively.

2.2 Modeling Recurrent Neural Networks to Predict $PM_{2.5}$

The fundamental issue of vanishing gradients frequently affects basic RNNs. By utilizing a gate concept, which has already been utilized in numerous research as a representative RNN cell, Long-term Short-Term Memory (LSTM) methods and TensorFlow might solve this problem.

Table 1. The RNN model uses observational input variables. The descending order of the correlation coefficients (R) between the input variable and the observed $PM_{2.5}$ is shown.

Variable Name	Description	Range
O_PRCP	6-h accumulated precipitation	− 0.068
O_U	Zonal wind	− 0.133
O_V	Meridional wind	0.205
O_RH	Relative humidity	0.362
O_Ta	Air temperature	0.368
O_SO_2	Sulfur dioxide	0.443
O_Td	Dew point temperature	0.467
O_NO_2	Nitrogen dioxide	0.518
O_PM_{10}	Particulate matter (aerodynamic diameters ≤10 μm)	0.591
O_CO	Carbon monoxide	0.68
O_$PM_{2.5}$	Particulate matter (aerodynamic diameters ≤2.5 μm)	1.000

Table 2. Similar to Table 1, but with input variables derived from numerical model results.

Variable Name	Description	Range
CP_2	2nd clustering pattern probability	0.040
CP_3	3rd clustering pattern probability	− 0.055
CP_4	4th clustering pattern probability	0.065
CP_5	5th clustering pattern probability	− 0.089
CP_1	1st clustering pattern probability	0.112
C_U_{500}	Cosine similarity of horizontal wind at 500 hPa	0.306
C_V_{700}	Cosine similarity of meridional wind at 700 hPa	0.311
C_T_{850}	Cosine similarity of air temperature at 850 hPa	0.312
V_{850}	Meridional wind at 850 hPa	0.320
Z_{700}	Geopotential height at 700 hPa	0.327
T	Air temperature at surface	0.350
C_Z_{500}	Cosine similarity of geopotential height at 500 hPa	0.352
SO_2	Sulfur dioxide	0.352
O_3	Ozone	− 0.369
C_W_{850}	Cosine similarity of vertical wind at 850 hPa	0.371
T_{850}	Air temperature at 850 hPa	0.383
RH	Relative humidity	0.384
NO_2	Nitrogen dioxide	0.405
CO	Carbon monoxide	0.634
PM_{10}	Particulate matter (aerodynamic diameters ≤10 μm)	0.654
$PM_{2.5}$	Particulate matter (aerodynamic diameters ≤2.5 μm)	0.655

The following Eqs. (1)–(6) define the LSTM:

$$i_t = \sigma\,(y_t W_{xi} + a_{xi} + h_{t-1} W_{hi} + a_{hi})$$

$$p_t = \sigma\,(y_t W_{xf} + a_{xf} + h_{t-1} W_{hf} + a_{hf})$$

$$o_t = \sigma\,(y_t W_{xo} + a_{xo} + h_{t-1} W_{ho} + a_{ho})$$

$$g_t = \sin\,(y_t W_{xg} + a_{xg} + h_{t-1} W_{hg} + a_{hg})$$

$$c_t = (p_t \odot c_{t-1} + i_t \odot g_t)$$

$h_t = o_t \odot sin\ (c_t)$

Where x_t, c_t, and ht refer to input data, cell state, and hidden state, respectively, at time *t*; i_t, *pt*, o_t, and g_t signify the input gate, forget gate, output gate, and cell gate, respectively, at the t-th time-step; Weight matrices are the W terms; b terms are bias vectors; the connections between the input and the four gates are denoted by the subscripts x_i, x_p, x_o, and x_g; the connections between the hidden states and the four gates are denoted by the subscripts hi, hf, h_o, and h_g; Sin is the sinusoidal activation function, and denotes an element-wise multiplication. Sig is the sigmoid activation function.

The LSTM's internal structure and workings are shown in Figure. 2. As shown in Figure 2, the forget, input, cell, and output gates receive the input signal at the t-th time step (x_t; blue circle) and the hidden state at the t-1-th time step (ht-1; gray dashed circle) (yellow boxes in Fig. 2). The cell state and hidden state signals are transmitted at the t-th time-step by multiplying and summing the signals from the activation functions of the four gates and the cell state at the previous time-step (ct-1; gray circle in Fig. 2) (ct and ht, respectively). How much old knowledge (ct-1) will be forgotten is determined by the forget gate. The information to be updated in the new cell state is determined by the input and cell gate (ct). The amount of transition from cell state to hidden state (ht) that will propagate to the following timestep (i.e., the t+1-th step) is decided by the output gate.

An input layer, three hidden layers (two stacked LSTM and fully connected layers), and an output layer make up the RNN model (Fig. 1). The two LSTM layers are connected to the input layer (blue boxes in Fig. 1) and are continually connected in accordance with the time-steps. The completely connected layer and output layer (pink and orange boxes in Fig. 1, respectively) are linked to the LSTM at the target prediction time to predict $PM_{2.5}$. 15 time-steps (T1-T15) of input data are spaced out over a period of 6 hours. In respect to the predicted start time, from 24 h (T1) to +60 h (T15) (T5). The T1-T5 phases included the observational data, as you can see. The time-steps in the prediction period between T6 and T15 are where the numerical model data are assigned. The T8-T11 and T12-T15 forecasts are employed in this study since the prediction start time (T5) is 12:00 local time, and they correspond to one-day (Day+1) and two-day (Day+2) forecasts, respectively. In each of the four districts, separate RNN models were created for the Day+1 and Day+2 forecasts. The differences between the districts that we looked at utilizing the TensorFlow were not very substantial (not shown). As a result, this paper will only offer the average results from the four districts.

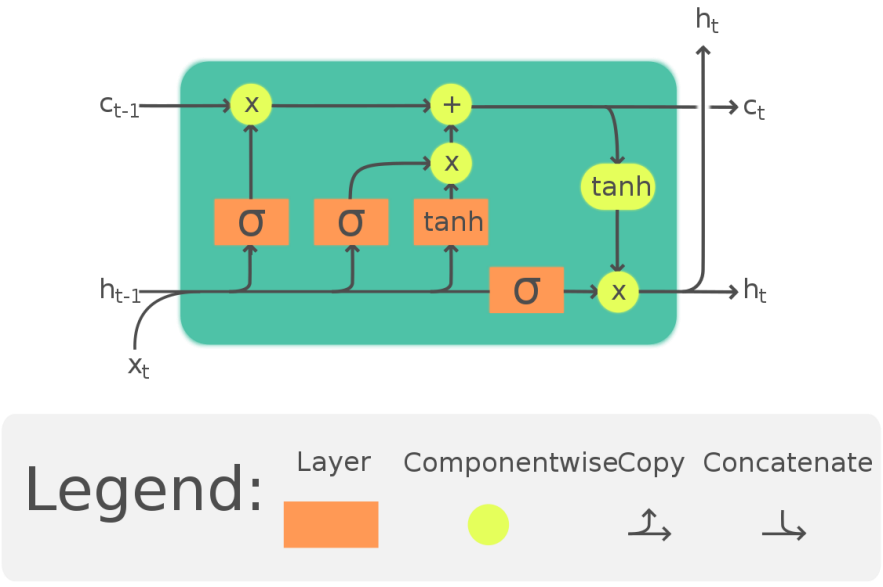

Figure 2. LSTM Structure
(Source: Wikipedia)

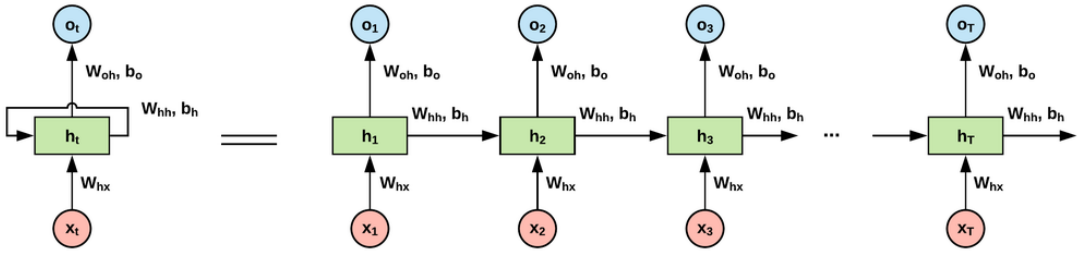

Figure 3. TensorFlow Model
(Source: www.easy-tensorflow.com)

The training (2021), validation (2021), and test (2022) periods were each given a set of data covering the whole time frame. The minimum and maximum values of the training set were used to normalize all three datasets. The $PM_{2.5}$ concentration and its level of hazard were evaluated. Low ($PM_{2.5}$ 16 µgram/m^3), moderate (16 µgram/m_3 36 µgram/$m^>$), high (36 µgram/m^3 76 µgram/m^3 $PM_{2.5}$), and extremely high (76 µgram/m^3 $PM_{2.5}$) were the categories used to characterize the levels of $PM_{2.5}$ concentrations. The correlation coefficient, mean bias error, and mean absolute error are used to evaluate $PM_{2.5}$ concentrations (R). The skill scores for accuracy, probability of detection (POD), and false alarm rate (FAR) for high and extremely high levels of $PM_{2.5}$ were used to evaluate the levels.

2.3 Tensorflow for Air Quality

The fundamental idea behind TensorFlow is to use backpropagation to assign relevance scores, which express a neuron's contribution to the output of the network, to every neuron in every layer of a neural network. Neurons in the immediate lower layer receive a redistribution of the relevance score from neurons in the upper layer. To meet the conservation property, as given in Eq. (7) below, the sum of the relevance scores in each layer should equal the output.

$$\text{Output Model} = \sum_i \quad R_i^I \quad = \sum_j \quad R_j^{I-1} \quad = \sum_k \quad R_k^{I-1}$$

Where the *i*-th neuron in the *I*-th layer's relevance score is R_i^I. From the input layer to the output layer, this relationship upholds the conservation law. Here, the output layer's relevance score is identical to the output itself. Iterating the decomposition process from the output layer to the input layer will allow you to determine the relevance scores of the other layers. Given the relevance score $R_k^{(I+1)}$ of the *k*-th neuron at the *I*+1-th layer, the relevance score R_j^I of the *j*-th neuron at the preceding layer is computed in two sequential layers *I*- and *I*+1-th.

$$R_{j\leftarrow k}^{(I,I+1)} = \frac{Z_j \times W_{jk} + \varepsilon \times sign(Z_k) + \delta \times b_k)/N}{Z_k + \varepsilon \times sign(Z_k)} R_k^{(I+1)}$$

$$R_k^{(I)} = \sum_k \quad R_{j\leftarrow k}^{(I,I+1)}$$

Z_k and Z_j are the node values in the two neurons, W_{jk} is the weight matrix that connects the two neurons, bk is the bias, is the stabilizer, is a multiplicative factor, and N is the number of neurons in the lower layer. $R_{j\leftarrow k}^{(I,I+1)}$ stands for the relevance propagation flow from the k-th neuron of the l+1-th layer to the j-th neuron of the For positive values, the sign(Z_j) is set to 1, while for negative values, it is set to 1.

A schematic representation of the relevance propagation procedures in the RNN model is shown in Fig. 2. Through relevance propagation (Eqs. (8) and (9); dashed box in Fig. 1), the

anticipated $PM_{2.5}$ concentration at the target prediction time (TP; orange box in Fig. 1) was divided into the relevance scores of the neurons in all layers. The relevance scores for all input variables at all timesteps in the input layer can be computed as the relevance propagation from the output layer reaches the input layer (blue dashed circles in Fig. 1). The relevance ratings for each timestep and each variable were added up in order to determine the time-steps and variables that had a significant impact on the $PM_{2.5}$ prediction. The total relevance score for each prediction is 1, as the relevance value was normalized by the projected $PM_{2.5}$ concentration.

3. Findings

3.1 Prediction of $PM_{2.5}$ With Input Time-Steps and Variables

The influence of each input variable in forecasting the $PM_{2.5}$ concentration was assessed at each input time-step in order to better understand the RNN model's decision-making process. The average relevance scores for the Day+1 (T8–T11, Fig. 5) and Day+2 (T12–T15, Fig. 5) forecasts are shown in Fig. 5 at each time-step from T1 to the target prediction time. To forecast the $PM_{2.5}$ concentration at T8, for example, the input variables from the observations for T1 through T5 and those from the numerical models for T6 through T8 are both employed, and the relevance scores at each time-step are calculated from T1 through T8 (dark red bars in Fig. 5). At the target prediction time and two to three time steps prior to it (for example, T5 to T8 for T8 prediction), the magnitude of the relevance score is typically large. At the goal prediction time and two time steps before to it, the relevance ratings for the Day+1 forecast are greater than 0. (Fig. 5). For the Day+2 forecast, the scores from the target prediction time to three time-steps before it are greater than 0.15. (Fig. 5). As the input time-steps approach further away from the goal forecast time, the relevance scores drop off quickly.

Description:

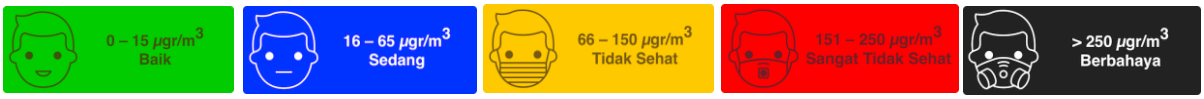

Figure 4 Threshold Value (NAV)
(Source: https://www.bmkg.go.id/)

In Fig. 4 describes the Threshold Value (NAV) Starting from 0 > 250 gram/m3 as the limit for air pollution concentrations. There are 5 colors with different meanings, starting from; (1) Green which means good, (2) Blue which means moderate, (3) Yellow which means unhealthy, (4) Red which means very unhealthy, (5) Black which means dangerous.

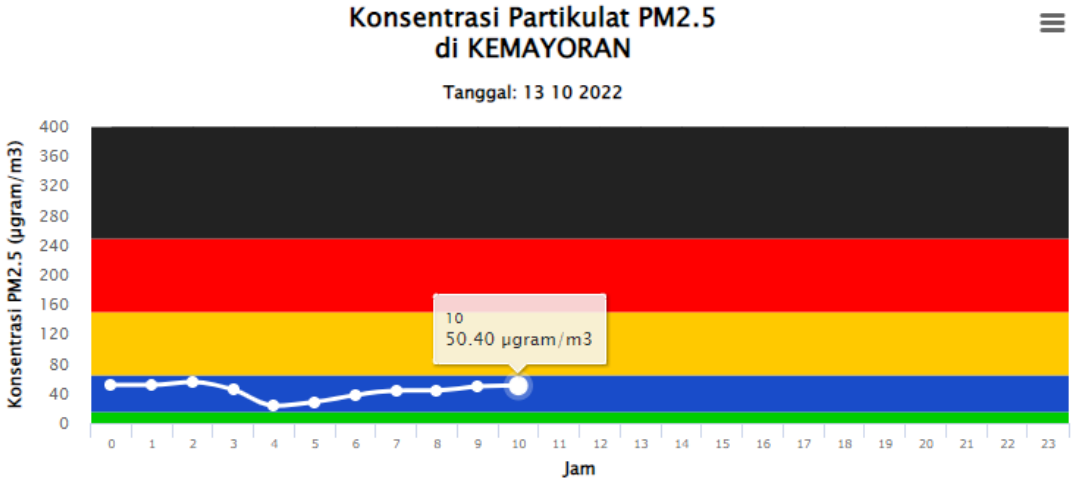

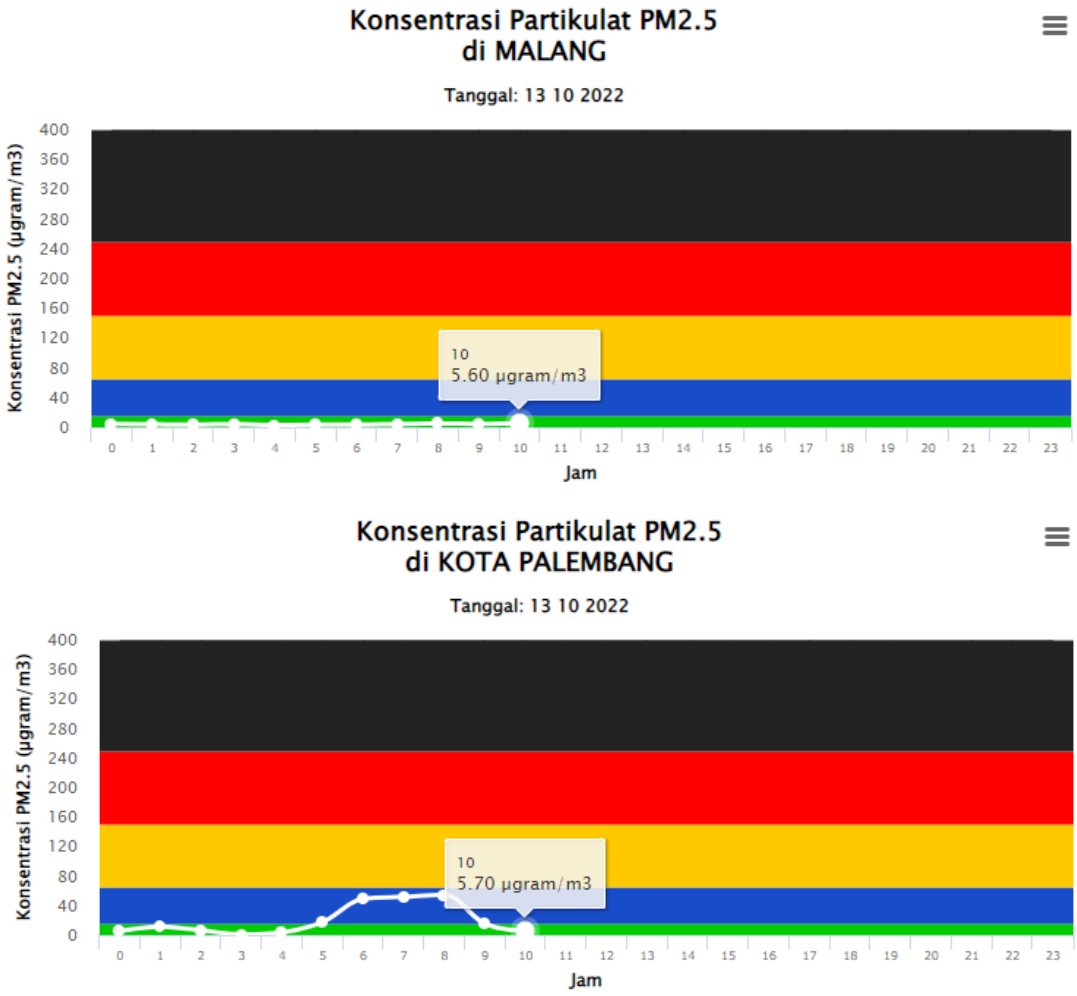

Figure 5. Concentration of Particulates ($PM_{2.5}$) in some parts of Indonesia (Source: https://www.bmkg.go.id/)

It is unlikely, according to Fig. 5, that the observational input factors from T1 to T5 considerably influence the $PM_{2.5}$ prediction. The cumulative ratio of each time-relevance step's score magnitude to the target forecast time's overall score is shown in Fig. 5. Around the goal prediction time, the accumulated ratio rises quickly, and near T1, it rises gradually. The aggregated ratios from the goal prediction time to T6 for the Day+1 forecast range from 0.629 to 0.887 (on average 0.753), and they range from 0.804 to 0.963 for the Day+2 forecast (0.909 on average). This shows that as prediction time goes up, the RNN model depends increasingly on the input variables from the numerical models. Only T5 (the forecast start time) of the observational input time-steps displays a relevance score close to that of the input time-steps from the numerical models in the Day+1 forecast. This outcome appears to be connected to two factors. The information from the past time is not entirely transferred to the output by the RNN's LSTM, to start. Second, the weights of the nodes closest to the output are higher.

The contribution of a particular input variable to the model prediction is shown by the sum of the relevance scores for each variable. The average relevance scores for each variable over all time-steps for the Day+1 and Day+2 forecasts are shown in Fig. 5. The order of magnitude of the relevance ratings is indicated on the x-axis in Fig. 5. Observed carbon monoxide (CO), predicted SO2 and O3, and predicted $PM_{2.5}$ and PM_{10} from the CMAQ are classified in the bottom 10, respectively, from the standpoint of air quality. The cosine

similarity of the 850 hPa temperature (C T850) and 500 hPa geopotential height (C Z500), local relative humidity (RH), 850 hPa temperature (T850), and 700 hPa geopotential height (Z700) from the WRF are among the meteorological variables that are ranked in the top 10. Due to high $PM_{2.5}$ episodes in the winter, the high-pressure system mitigates the high frequency of CP3 and CP4 occurrences.

It is noteworthy that the rank of the relevance scores does not match the correlation coefficients between the input factors and the observed $PM_{2.5}$ (Tables 1 and 2). For example, CO's relevance score is insignificant as it only ranks 22nd, despite having a correlation coefficient that is greater than 0.6 and placing 5th overall. Although the correlation coefficient of C Z500 is ranked in the middle, the relevance score of C Z500 is also ranked third. Only 0.206 percent of the correlation coefficients and relevance ratings had a rank correlation. It should be emphasized that the input variables were chosen using correlation coefficients, as a variable with a high correlation coefficient is probably crucial for $PM_{2.5}$ forecasts. Due to their strong associations with $PM_{2.5}$, observational data, particularly air quality indices, would be crucial for prediction (Tables 1 and 2). Regardless of the correlation coefficients, the relevance ratings are distributed differently. This finding indicates a contradiction between the old method's linear notion (correlation coefficient) and the neural network's nonlinear concept (relevance score). As a result, it is challenging to understand how an AI model behaves using solely linear methods.

3.2 Using Significant Input Time-Steps and Variables, Prediction

The RNN model was retrained based on the relevance score result to determine whether the major time-steps and variables discovered by the TensorFlow play a significant role in the RNN model. Based on the time-steps and variables that accounted for 80% of the overall relevance score, the important time-steps and variables with high relevance scores have been chosen. We put the model to the test by using different cutoffs (85% and 90%) and found no discernible changes in the results. The time-steps T6 for the Day+1 forecast (white bar in Fig. 5) and T8 for the Day+2 forecast are those where the accumulated ratio from the goal prediction time is closest to 80%. (black bar in Fig. 5). Fig. 5 shows the cumulative ratio of each variable's relevance score magnitude to the sum from the first rank variable. Fig. 5 shows the cumulative ratio of each variable's relevance score magnitude to the sum from the first rank variable. Similar to this, the accumulated ratio rises quickly close to the first rank variable then gradually as the rank rises. For the Day+1 forecast (white bars in Fig. 5) and the Day+2 forecast (black bars in Fig. 5), the variable rank where the accumulated ratio from the first rank is closest to 80% is 13 and 15, respectively (black bars in Fig. 5). The time-steps from the T6 (T9) to the goal prediction time and the variables above the 13th (15th) rank, respectively, were chosen as the key input timesteps and variables for the Day+1 (Day+2) forecast.

Table 3 compares the Day+1 and Day+2 forecasting abilities of the CMAQ, original RNN, and retrained RNN models for the winters of 2015–2021. The major input time-steps and variables were used to retrain the RNN model, which was given the names RNN T and RNN V, respectively. The retrained RNN models decrease MAE by 6.9 g/m^3 and 7.1 g/m^3 and MBE by 8.9 g/m^3 in both cases when compared to CMAQ, respectively. The retrained RNN models outperform the CMAQ forecasts in terms of accuracy and FAR by 18.4%, 19.3%, and 18.9%, respectively. Since the CMAQ projections overestimate the concentration of $PM_{2.5}$, they produce larger POD than RNN models. As a result, compared to the CMAQ model, the retrained RNN models' prediction abilities are considerably closer to those of the original RNN model. Furthermore, compared to the original model's POD (75.0%), the retrained RNN models' PODs are 4.1% and 3.8% higher. This finding emphasizes the value of the TensorFlow approach in comprehending the RNN model by confirming that the major input time-steps and variables proposed by the TensorFlow method play a significant influence in forecasting $PM_{2.5}$.

4. Conclusion

Using the TensorFlow approach, a representative XAI technique where relevance scores are delivered to each neuron of all layers in the RNN by backpropagation beginning at the output layer, this study seeks to understand the decision-making process of an RNN model for $PM_{2.5}$ prediction in the Tangerang metropolitan area of Indonesia. To determine the contribution of the input layer to the prediction, the relevance scores for the input time-steps and variables were examined. According to the time-step analysis, the input variables from the numerical models (CMAQ and WRF) are crucial for forecasting $PM_{2.5}$ concentrations. For the Day+1 and Day+2 forecasts, in particular, input time-steps from the target prediction time to T6 and T8 account for over 80% of the overall relevance score. The study of each input variable reveals that, for the Day+1 and Day+2 forecasts, respectively, the top-13 and top-15 relevance score factors accounted for over 80% of the total score. The $PM_{2.5}$ and PM10 simulated by the CMAQ and the observed $PM_{2.5}$ made the biggest contributions to the RNN model's prediction among the air quality variables. The cosine similarity of the 850 hPa temperature and 500 hPa geopotential height, as well as the local relative humidity, 850 hPa temperature, and 700 hPa geopotential, were the meteorological variables with the highest relevance scores. By retraining the RNN model with the key input time-steps and variables that make up 80% of the total score, the TensorFlow results were validated. It is confirmed that the input time-steps and variables chosen by the TensorFlow approach considerably contribute to the prediction when the prediction accuracy of the retrained RNN models does not significantly differ from that of the original model.

The RNN model's prediction error may be studied using the TensorFlow approach. For instance, by concentrating on the significant time-steps and variables with high relevance scores obtained by the TensorFlow approach, the sources of mistakes can be successfully analyzed. Additionally, it is confirmed that the numerical models' input data play a key role in determining how well the RNN model predicts (Figs. 4 and 5). Generally speaking, as the prediction lead time is extended, the numerical model's predictive ability declines; this is also shown in the forecasts produced by the RNN model. As a result, the numerical model needs to be enhanced for the AI model's greater prediction abilities.

In contrast to the linear connections between the input variables and $PM_{2.5}$, the relevance scores of the input variables are distributed unevenly in the RNN model. This suggests that AI models may use a decision-making process that is challenging to explain using our current understanding or simple linear ideas. A deeper knowledge of the mechanisms linked to $PM_{2.5}$ concentration, which continue to be a key issue for this field of research, will be needed in order to comprehend the drivers for decision-making in AI models.

Acknowledgment

The author would like to thank the Alphabet Incubator Center of Excellence and University of Raharja for the support in developing and improving this article. And funding for Research and Higher Education PKM for Fiscal Year 2022 Referring to Letter Number 0357/E5/AK.04/2022 from the Ministry of Education, Culture, Research, and Technology.

References

[1] R. Yunita, M. S. Shihab, D. Jonas, H. Haryani, and Y. A. Terah, “Analysis of The Effect of Servicescape and Service Quality on Customer Satisfaction at Post Shop Coffee Tofee in Bogor City,” *Aptisi Trans. Technopreneursh.*, vol. 4, no. 1, pp. 68–76, 2022.

[2] N. K. A. Dwijendra *et al.*, “Application of Experimental Design in Optimizing Fuel Station Queuing System,” *Ind. Eng. Manag. Syst.*, vol. 21, no. 2, pp. 381–389, 2022.

[3] D. P. Lazirkha, “The impact of artificial intelligence in smart city air purifier systems,” *Aptisi Trans. Technopreneursh.*, vol. 4, no. 2, pp. 205–214, 2022.

[4] D. Kim, C.-H. Ho, I. Park, J. Kim, L.-S. Chang, and M.-H. Choi, “Untangling the contribution of input parameters to an artificial intelligence PM2. 5 forecast model using the layer-wise relevance propagation method,” *Atmos. Environ.*, vol. 276, p. 119034,

2022.
[5] Q. Aini, W. Febriani, C. Lukita, S. Kosasi, and U. Rahardja, “New Normal Regulation with Face Recognition Technology Using AttendX for Student Attendance Algorithm,” in *2022 International Conference on Science and Technology (ICOSTECH)*, 2022, pp. 1–7.
[6] P.-Y. Kow *et al.*, “Seamless integration of convolutional and back-propagation neural networks for regional multi-step-ahead PM2. 5 forecasting,” *J. Clean. Prod.*, vol. 261, p. 121285, 2020.
[7] O. Octaria, D. Manongga, A. Iriani, H. D. Purnomo, and I. Setyawan, “Mining Opinion Based on Tweets about Student Exchange with Tweepy and TextBlob,” in *2022 9th International Conference on Information Technology, Computer, and Electrical Engineering (ICITACEE)*, 2022, pp. 102–106.
[8] U. Rahardja, P. A. Sunarya, N. Lutfiani, M. Hardini, and S. N. Sari, “Transformation of green economic recovery based on photovoltaic solar canopy,” *Transformation*, vol. 7, no. 2, 2022.
[9] C.-C. Huang, M.-J. Chang, G.-F. Lin, M.-C. Wu, and P.-H. Wang, “Real-time forecasting of suspended sediment concentrations reservoirs by the optimal integration of multiple machine learning techniques,” *J. Hydrol. Reg. Stud.*, vol. 34, p. 100804, 2021.
[10] P. A. Sunarya, “Penerapan Sertifikat pada Sistem Keamanan menggunakan Teknologi Blockchain,” *J. MENTARI Manajemen, Pendidik. dan Teknol. Inf.*, vol. 1, no. 1, pp. 58–67, 2022.
[11] M. R. Pribadi, D. Manongga, H. D. Purnomo, and I. Setyawan, “Sentiment Analysis of the PeduliLindungi on Google Play using the Random Forest Algorithm with SMOTE,” in *2022 International Seminar on Intelligent Technology and Its Applications (ISITIA)*, 2022, pp. 115–119.
[12] P. Partheeban, “Application of LSTM Models in Predicting Particulate Matter (PM2. 5) Levels for Urban Area,” *J. Eng. Res.*, 2021.
[13] E. S. Pramono, D. Rudianto, F. Siboro, M. P. A. Baqi, and D. Julianingsih, “Analysis Investor Index Indonesia with Capital Asset Pricing Model (CAPM),” *Aptisi Trans. Technopreneursh.*, vol. 4, no. 1, pp. 36–47, 2022.
[14] M. Vössing, N. Kühl, M. Lind, and G. Satzger, “Designing Transparency for Effective Human-AI Collaboration,” *Inf. Syst. Front.*, pp. 1–19, 2022.
[15] V. Elmanda, A. E. Purba, Y. P. A. Sanjaya, and D. Julianingsih, “Efektivitas Program Magang Siswa SMK di Kota Serang Dengan Menggunakan Metode CIPP di Era Adaptasi New Normal Pandemi Covid-19,” *ADI Bisnis Digit. Interdisiplin J.*, vol. 3, no. 1, pp. 5–15, 2022.
[16] D. Gunning, “Explainable artificial intelligence (xai),” *Def. Adv. Res. Proj. agency (DARPA), nd Web*, vol. 2, no. 2, p. 1, 2017.
[17] D. Julianingsih, A. G. Prawiyogi, E. Dolan, and D. Apriani, “Utilization of Gadget Technology as a Learning Media,” *IAIC Trans. Sustain. Digit. Innov.*, vol. 3, no. 1, pp. 43–45, 2021.
[18] A. Holzinger, B. Malle, A. Saranti, and B. Pfeifer, “Towards multi-modal causability with graph neural networks enabling information fusion for explainable AI,” *Inf. Fusion*, vol. 71, pp. 28–37, 2021.
[19] B. P. K. Bintoro, N. Lutfiani, and D. Julianingsih, “Analysis of the Effect of Service Quality on Company Reputation on Purchase Decisions for Professional Recruitment Services,” *APTISI Trans. Manag.*, vol. 7, no. 1, pp. 35–41, 2023.
[20] D. Minh, H. X. Wang, Y. F. Li, and T. N. Nguyen, “Explainable artificial intelligence: a comprehensive review,” *Artif. Intell. Rev.*, pp. 1–66, 2021.
[21] B. Pang, E. Nijkamp, and Y. N. Wu, “Deep learning with tensorflow: A review,” *J. Educ. Behav. Stat.*, vol. 45, no. 2, pp. 227–248, 2020.
[22] H. Wu, A. Huang, and J. W. Sutherland, “Layer-wise relevance propagation for interpreting LSTM-RNN decisions in predictive maintenance,” *Int. J. Adv. Manuf. Technol.*, vol. 118, no. 3, pp. 963–978, 2022.
[23] N. K. A. Dwijendra *et al.*, “An Analysis of Urban Block Initiatives Influencing Energy Consumption and Solar Energy Absorption,” *Sustainability*, vol. 14, no. 21, p. 14273, 2022.
[24] I. Ruhiyat, L. Meria, and D. Julianingsih, “Peran Pelatihan dan Keterikatan Kerja Untuk

Meningkatkan Kinerja Karyawan Pada Industri Telekomunikasi," *Technomedia J.*, vol. 7, no. 1, pp. 90–110, 2022.
[25] M. A. Myszczynska *et al.*, "Applications of machine learning to diagnosis and treatment of neurodegenerative diseases," *Nat. Rev. Neurol.*, vol. 16, no. 8, pp. 440–456, 2020.
[26] A. Williams, R. Widayanti, T. Maryanti, and D. Julianingsih, "Effort To Win The Competition In Digital Business Payment Modeling," *Startupreneur Bisnis Digit.*, vol. 1, no. 1 April, pp. 84–96, 2022.
[27] D. Kim, S. Cho, L. Tamil, D. J. Song, and S. Seo, "Predicting asthma attacks: effects of indoor PM concentrations on peak expiratory flow rates of asthmatic children," *IEEE Access*, vol. 8, pp. 8791–8797, 2019.
[28] V. Agarwal, M. C. Lohani, A. S. Bist, and D. Julianingsih, "Application of Voting Based Approach on Deep Learning Algorithm for Lung Disease Classification," in *2022 International Conference on Science and Technology (ICOSTECH)*, 2022, pp. 1–7.
[29] U. Rahardja, V. T. Devana, N. P. L. Santoso, F. P. Oganda, and M. Hardini, "Cybersecurity for FinTech on Renewable Energy from ACD Countries," in *2022 10th International Conference on Cyber and IT Service Management (CITSM)*, 2022, pp. 1–6.
[30] R. Chalapathy, N. L. D. Khoa, and S. Sethuvenkatraman, "Comparing multi-step ahead building cooling load prediction using shallow machine learning and deep learning models," *Sustain. Energy, Grids Networks*, vol. 28, p. 100543, 2021.
[31] G. Maulani, N. Wiwin, V. Elmanda, and D. Julianingsih, "Conscious Fog and Electricity Computing Performance: Renewable Energy Case Study," in *2022 International Conference on Science and Technology (ICOSTECH)*, 2022, pp. 1–7.
[32] U. Rahardja, "Blockchain Education: as a Challenge in the Academic Digitalization of Higher Education," *IAIC Trans. Sustain. Digit. Innov.*, vol. 4, no. 1, pp. 62–69, 2022.
[33] G. Nguyen *et al.*, "Machine learning and deep learning frameworks and libraries for large-scale data mining: a survey," *Artif. Intell. Rev.*, vol. 52, no. 1, pp. 77–124, 2019.
[34] W. Sejati, D. P. AH, F. Khansa, A. S. Maulana, and D. Julianingsih, "Flood Disaster Mitigation Using the HEC-RAS Application to Determine River Water Levels in the Old City Area of Jakarta," *Aptisi Trans. Technopreneursh.*, vol. 4, no. 2, pp. 121–134, 2022.
[35] Q. Aini, D. Manongga, U. Rahardja, I. Sembiring, and R. Efendy, "Innovation and Key Benefits of Business Models in Blockchain Companies," *Blockchain Front. Technol.*, vol. 2, no. 2, pp. 24–35, 2023.